Mitogenic stimulation accelerates influenza-induced mortality by increasing susceptibility of alveolar type II cells to infection

Nikolaos M. Nikolaidis[a,1], John G. Noel[b], Lori B. Pitstick[a], Jason C. Gardner[a,b], Yasuaki Uehara[a], Huixing Wu[a], Atsushi Saito[a,2], Kara E. Lewnard[a], Huan Liu[a], Mitchell R. White[c], Kevan L. Hartshorn[c], and Francis X. McCormack[a,1]

[a]Department of Internal Medicine, Division of Pulmonary, Critical Care, and Sleep Medicine, University of Cincinnati College of Medicine, Cincinnati, OH 45267; [b]Department of Research, Shriner's Hospital for Children, Cincinnati, OH 45229; and [c]Department of Medicine, Boston University School of Medicine, Boston, MA 02118

Edited by Peter Palese, Icahn School of Medicine at Mount Sinai, New York, NY, and approved June 29, 2017 (received for review December 23, 2016)

Development of pneumonia is the most lethal consequence of influenza, increasing mortality more than 50-fold compared with uncomplicated infection. The spread of viral infection from conducting airways to the alveolar epithelium is therefore a pivotal event in influenza pathogenesis. We found that mitogenic stimulation with keratinocyte growth factor (KGF) markedly accelerated mortality after infectious challenge with influenza A virus (IAV). Coadministration of KGF with IAV markedly accelerated the spread of viral infection from the airways to alveoli compared with challenge with IAV alone, based on spatial and temporal analyses of viral nucleoprotein staining of lung tissue sections and dissociated lung cells. To better define the temporal relationship between KGF administration and susceptibility to IAV infection in vivo, we administered KGF 120, 48, 24, and 0 h before intrapulmonary IAV challenge and assessed the percentages of proliferating and IAV-infected, alveolar type II (AECII) cells in dispersed lung cell populations. Peak AECII infectivity coincided with the timing of KGF administration that also induced peak AECII proliferation. AECII from mice that were given intrapulmonary KGF before isolation and then infected with IAV ex vivo exhibited the same temporal pattern of proliferation and infectious susceptibility. KGF-induced increases in mortality, AECII proliferation, and enhanced IAV susceptibility were all reversed by pretreatment of the animals with the mTOR inhibitor rapamycin before mitogenic stimulation. Taken together, these data suggest mTOR signaling-dependent, mitogenic conditioning of AECII is a determinant of host susceptibility to infection with IAV.

viral pneumonia | influenza A | alveolar epithelial type II | mitogen | mTOR

Influenza virus spreads across the globe in seasonal epidemics that cause 3–5 million cases of severe illness and claim up to 500,000 lives each year (1–3). In most patients, influenza symptoms last 7–10 d and are limited to fever, rhinitis, pharyngitis, myalgias, headache, and cough resulting from viral bronchitis (4). Although individual risk for mortality is low, a significant subset of infected patients develop pneumonia, the most lethal consequence of influenza (5). Those at the highest risk for infection and complications include pregnant women (6), the elderly (>65 y) (7), the very young (<5 y of age, and especially less than 2 y), smokers (8), those exposed to inhaled toxicants such as oxygen (9) and air pollutants (10), and patients with chronic illnesses such as diabetes and emphysema (11, 12). Increased risk is often ascribed to impairment of the immune system, and differential susceptibility of the airway epithelium is seldom considered in mechanistic studies of host factors that predispose to IAV infection and poor outcomes. An understanding of the epithelial factors that promote the spread of influenza from the conducting airway to the alveolar compartment, leading to progression from bronchitis to pneumonia, would greatly facilitate the development of strategies to lessen the effect of influenza infection.

On inhalation into the respiratory tract, influenza virus affects the nasal, oropharyngeal, and upper airway epithelium. Receptors at the apex of abundant trimeric hemagglutinin (HA) proteins jutting from the viral envelope bind to terminal sialic acid residues on glycoproteins and glycolipids of host cells, promoting internalization of the virions by endocytosis (13). Proteolytic cleavage of the HA by soluble and membrane-bound enzymes facilitates a key conformational change that mediates fusion of the viral and endosomal envelopes (14). This process is aided by viral pore (M2) proteins, which facilitate endosomal acidification and drive the release of core proteins and viral RNA into the cytoplasm, which are then transported into the nucleus (15). There, host replication machinery is coopted to produce viral RNA and protein that are packaged into new viral particles and transported to the cell surface (16). Neuraminidase cleaves the sialic acid link between the viral HA and cell surface glycans that tether the virus to the host cell, liberating viral progeny to perpetuate the infectious cycle (17, 18).

The pulmonary collectins, surfactant proteins A (SP-A) and D (SP-D), are pulmonary epithelium-derived host defense proteins that have been previously reported to bind to HA and opsonize and agglutinate IAV (19–24). Keratinocyte growth factor (KGF), a potent epithelial mitogen and differentiation factor, has been shown to increase pulmonary collectin expression, promote epithelial

Significance

Influenza is a recurring global health threat that preferentially targets vulnerable groups such as the very young, the pregnant, the elderly, and the infirm. The spread of influenza A virus (IAV) from the epithelium of the conducting airway to the alveolar epithelium is a pivotal event in the pathogenesis of primary viral pneumonia. Host susceptibility to IAV pneumonia is often attributed to altered immunity, and cell autonomous vulnerability states of the alveolar epithelium, such as proliferative tone, are rarely considered. Here we demonstrate that mitogenic stimulation of alveolar epithelial type II cells renders them susceptible to IAV infection in an mTOR-dependent manner.

Author contributions: N.M.N., J.G.N., L.B.P., J.C.G., H.W., K.E.L., M.R.W., K.L.H., and F.X.M. designed research; N.M.N., J.G.N., L.B.P., J.C.G., Y.U., H.W., A.S., K.E.L., and H.L. performed research; N.M.N., J.G.N., J.C.G., K.E.L., and F.X.M. analyzed data; and N.M.N. and F.X.M. wrote the paper.

The authors declare no conflict of interest.

This article is a PNAS Direct Submission.

Freely available online through the PNAS open access option.

[1]To whom correspondence may be addressed. Email: nikolan@uc.edu or MCCORMFX@UCMAIL.UC.EDU.

[2]Present address: Department of Biochemistry, Sapporo Medical University, School of Medicine, Sapporo, Japan; and Department of Respiratory Medicine and Allergology, Sapporo Medical University, School of Medicine, Sapporo, Japan.

This article contains supporting information online at www.pnas.org/lookup/suppl/doi:10.1073/pnas.1621172114/-/DCSupplemental.

repair, and protect the lung from a variety of infectious and noninfectious insults (25–31). Our initial hypothesis in this study was that KGF administration would increase pulmonary collectin levels in the airspace and enhance the survival of mice challenged with IAV. We found instead that KGF accelerated the spread of virus from the conducting airways into the alveolar space and increased both viral burden and mortality through the cell autonomous enhancement of AECII susceptibility to viral infection.

Results

Intrapulmonary Administration of KGF Enhances Mortality and Viral Burden After Pulmonary IAV Challenge. Experiments were conducted to test the hypothesis that KGF administration would enhance survival of mice challenged with WSNHAnc-Asp225Gly (a SP-D–sensitive, hybrid IAV strain, WSNHAnc-Asp225Gly, hereafter referred to as IAV), and the results are shown in Fig. 1*A*. Animals were inoculated via the intratracheal (i.t.) route with a PBS solution containing 1,500 IAV particles with or without 5 mg/kg KGF, and vital status was followed over the course of 11 d. Although all animals ultimately succumbed to IAV infection, KGF coadministration shortened survival by an average of 3 d ($P = 0.01$). Coadministration of IAV with KGF at concentrations spanning 4 logs (0.1, 1, 10, and 100 μg/mouse) resulted in dose-dependent acceleration of mortality (Fig. 1*B*). Pretreatment with KGF 120 h before inoculation with IAV did not enhance mortality compared with mice given PBS/IAV at time 0 (Fig. 1*C*). Mice treated with concomitant i.t. IAV and KGF (5 mg/kg) had a three- to fivefold greater pulmonary viral burden by 48 and 72 h postchallenge compared with PBS/IAV-treated controls, based on real-time PCR of IAV RNA in whole-lung homogenates (Fig. 1*D*; $P < 0.01$). No difference in viral burden was detected between the PBS/IAV and KGF/IAV groups at the 24 h postinoculation point.

Effect of KGF and IAV on Inflammatory Profiles in BALF, Serum, and Whole-Lung Homogenates. To explore the role of inflammation in the KGF-augmented mortality of IAV-infected mice, we conducted a multiplex analysis of inflammatory mediators in serum and acellular broncho-alveolar lavage fluid (BALF) collected at 24 and 72 h after i.t. challenge with 1,500 viral particles of IAV in PBS with or without 5 mg/kg KGF (Fig. 2 *A* and *B* and Fig. S1). Changes in selected cytokines at 72 h postchallenge are shown as fold change from PBS controls. Coadministration of KGF with IAV modestly augmented BAL IP10, MCP-5, TNFα, MIG, IL-6, MCP-1, G-CSF, M-CSF, and IFNγ responses relative to the PBS/IAV control group. KGF also augmented the inflammatory response to IAV challenge in serum for some cytokines, especially for IP10, TNFα, MCP-1, and IFNγ. To confirm changes to pulmonary proinflammatory cytokines, levels of IL-6, TNFα, KC, and MCP-1 were also measured by ELISA in whole-lung homogenates at 24, 48, and 72 h after IAV challenge in the presence or absence of KGF (Fig. 2 *C*–*F*). IAV alone produced three- to eightfold increases in IL-6, TNFα, KC, and MCP-1 levels at 48 and 72 h, which were modestly enhanced (by ∼10–50%) by KGF coadministration. Control experiments were also performed to determine the effect of KGF treatment alone. There was no effect of KGF treatment alone on cytokine responses at any point, except for two- to threefold increases in TNFα at 48 and 72 h postchallenge (Fig. 2*D*) compared with naive controls.

KGF Promotes the Spread of Viral Infection from the Airways to the Lung Parenchyma. Experiments were conducted to determine the effects of KGF on the spatial and temporal pattern of pulmonary IAV infection. Influenza nucleoprotein (IAV-NP) staining was performed on inflation-fixed whole-lung sections (Fig. 3 *A* and *B*) at 48 and 120 h after i.t. inoculation of 1,500 viral particles of IAV, with and without KGF coadministration. At 48 h after viral

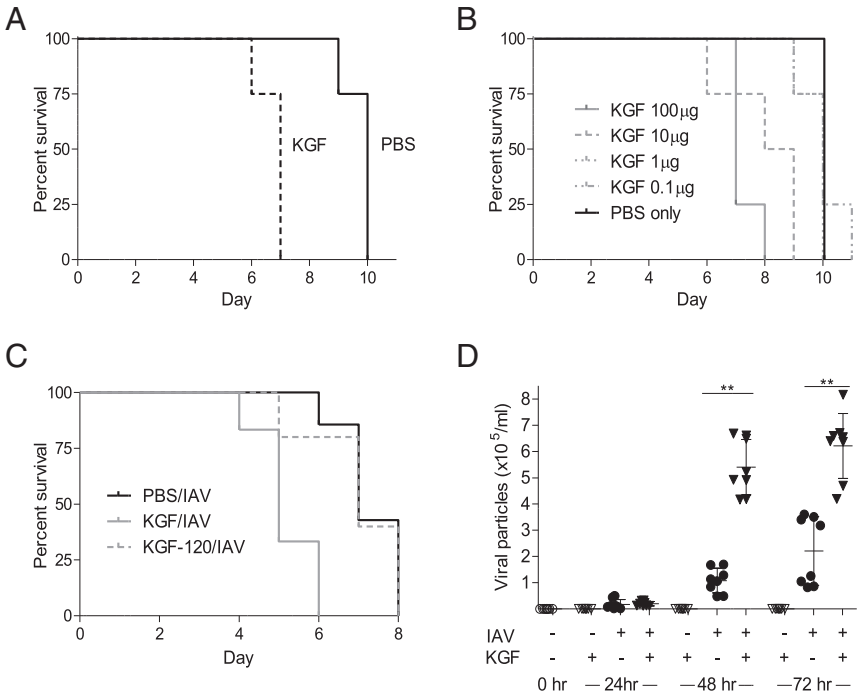

Fig. 1. KGF administration enhances IAV-induced mortality and viral burden. (*A*) Mice were given i.t. IAV (1,500 viral particles) in PBS with or without 5 mg/kg KGF, and vital status was monitored over the course of 11 d ($n = 4$/group; $P = 0.01$ for difference between PBS and KGF groups). (*B*) IAV (1,500 viral particles) in PBS containing 100, 10, 1, 0.1, or 0 μg KGF were administered to mice by the i.t. route, and vital status was monitored over the course of 11 d ($n = 4$/group; $P < 0.01$ for KGF 100 or 10 mg/kg vs. PBS control). (*C*) Mice were treated with i.t. PBS alone (black line) or PBS containing KGF (5 mg/kg) at time 0 (gray line) or 120 h (gray dashed line) before infection with IAV. Vital status was monitored for 10 d postinfection ($n = 4$/group; $^*P < 0.05$ for −120 h and 0 h groups). (*D*) PBS with or without IAV (1,500 viral particles) and with or without 5 mg/kg KGF was administered i.t., and viral particles were quantified in lung homogenates by real-time PCR at 0, 24, 48, and 72 h postinfection. $^{**}P < 0.01$.

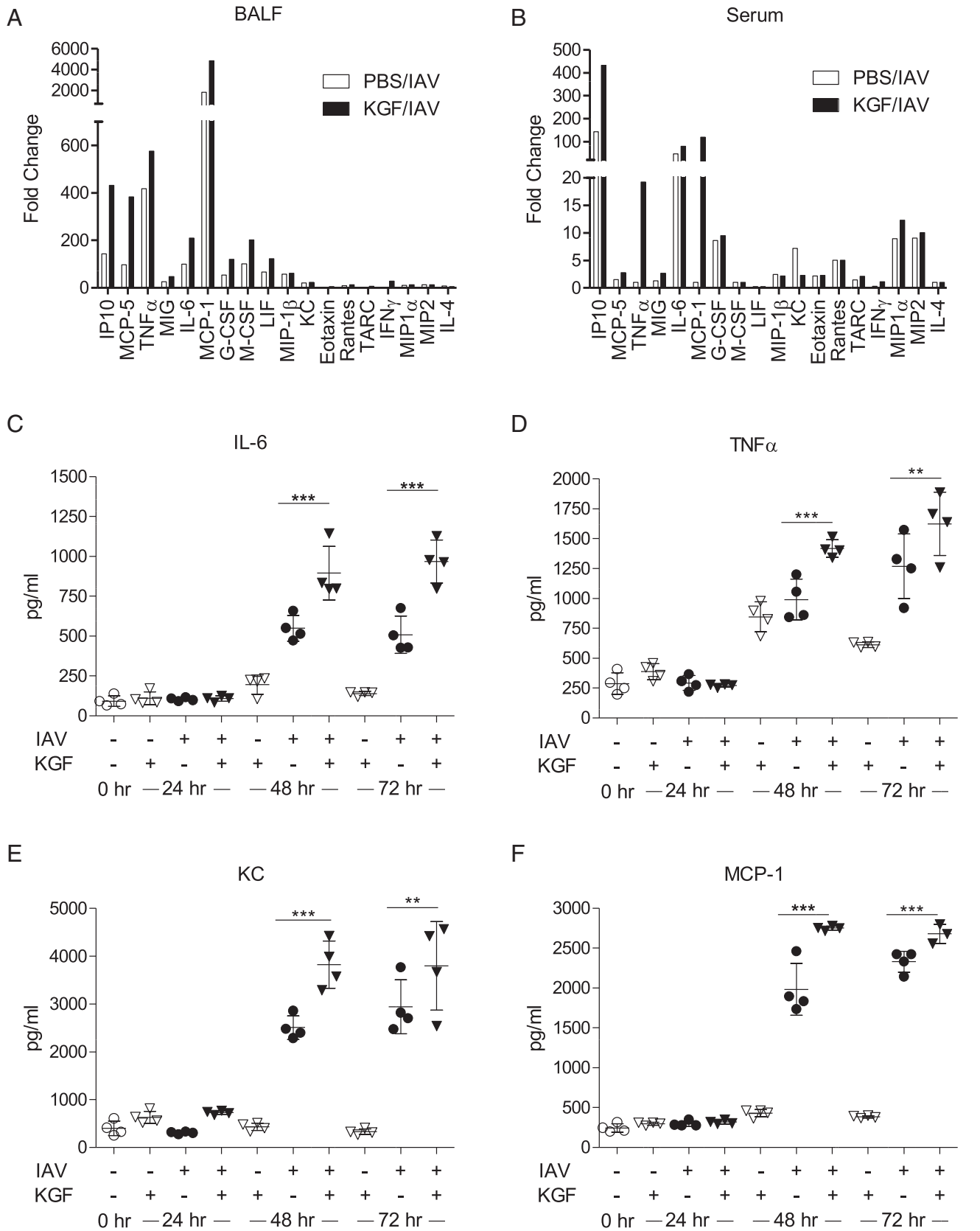

Fig. 2. Intrapulmonary KGF treatment increases IAV-induced proinflammatory cytokine levels. PBS with or without IAV (1,500 viral particles) and with or without 5 mg/kg KGF was administered i.t., and inflammatory cytokines were measured. (*A* and *B*) Multiplex analysis of 43 cytokines and chemokines was conducted 72 h later in acellular BALF and serum, respectively. Data in *A* and *B* were presented for most informative cytokines as fold change from PBS control (n = 3 mice/group). (*C*–*F*) IL-6, TNFα, KC (CXCL1), and MCP-1 (CCL2) levels were measured by ELISA in whole-lung homogenates at 0, 24, 48, and 72 h postinfection. ***$P < 0.001$; **$P < 0.01$.

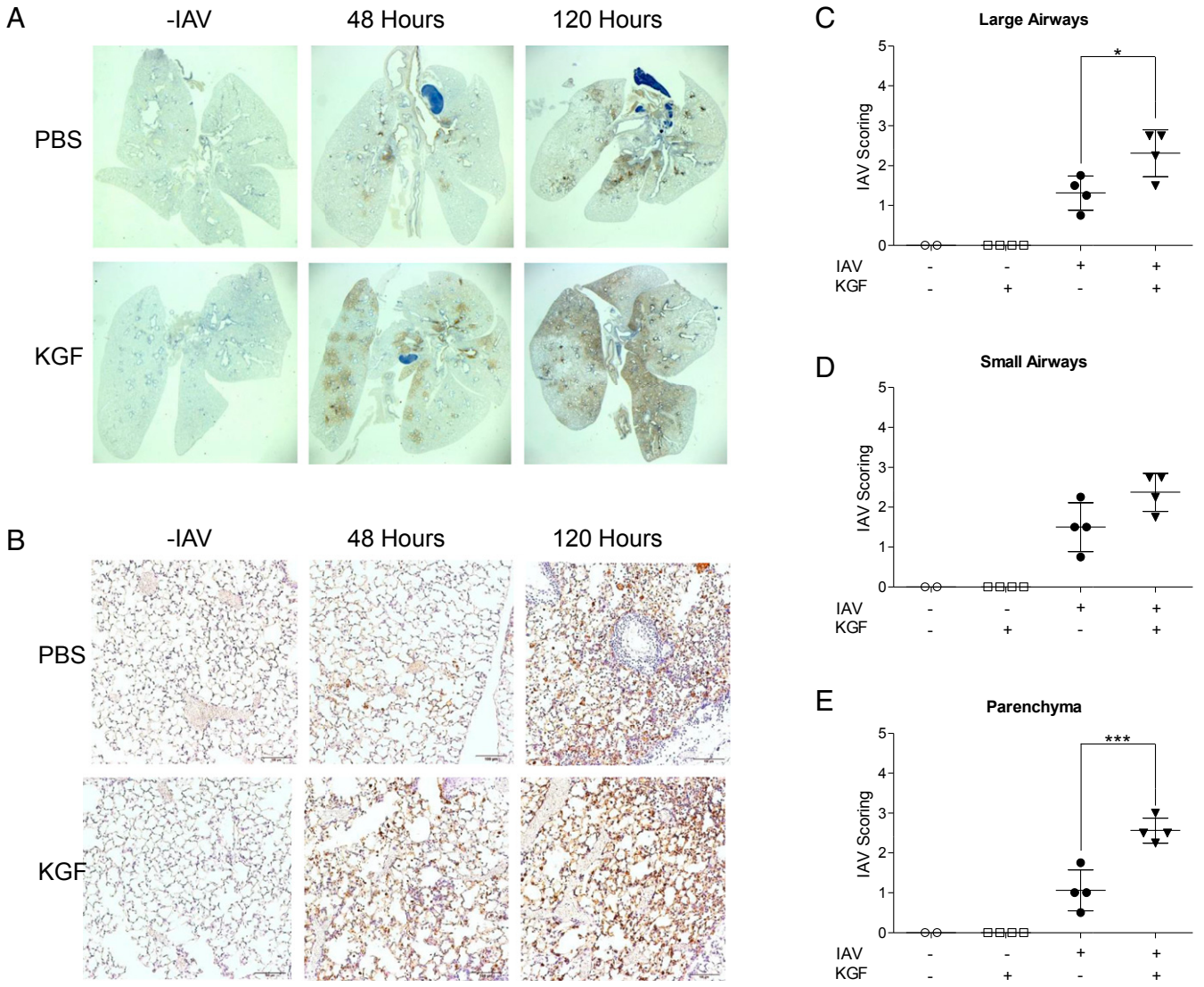

Fig. 3. IAV (1,500 viral particles) was administered in PBS with or without 5 mg/kg KGF. Lungs were inflation fixed and harvested at 0, 48, or 120 h. (*A* and *B*) Immunohistochemical staining for IAV-NP was performed on lung sections (bars, 200 μm). (*C–E*) IAV-NP staining of the 48-h lung sections was scored on a semiquantitative scale in a blinded manner. ***$P < 0.001$; *$P < 0.05$.

challenge, IAV-NP staining was faint and centered on large airways in mice that received only PBS with IAV. At the same time, in IAV-challenged mice given i.t. KGF, staining was substantially more intense, and extensive peribronchiolar spread into the surrounding lung parenchyma was readily apparent on both low-power (Fig. 3*A*) and high-power (Fig. 3*B*) views. By 120 h, IAV-NP staining was increased in both groups, but was markedly more intense and diffuse in the KGF group. Blinded semiquantitative analysis of IAV-NP staining in high-power lung sections was consistent with a KGF-induced increase in viral burden and acceleration of spread from conducting airways to the lung parenchyma (Fig. 3 *C–E*).

KGF-Enhanced AECII Infectivity Correlates with Their Proliferative State, in Vivo. Experiments were conducted to determine whether the mitogenic effects of KGF enhance the susceptibility of AECII to IAV infection in vivo. Single-cell suspensions were prepared from whole-lung homogenates 24 h after high-dose (50,000 viral particles) i.t. IAV challenge of mice that had been pretreated with i.t. KGF at 24, 48, or 120 h before infection (Fig. 4*A*). The dispersed cells were then washed, fixed, and stained with anti IAV-NP to detect IAV infection, anti-pro SP-C to identify AECII, and anti-Ki67, a marker of cellular proliferation. The percentage of AECII that were proliferating according to Ki67 staining increased in a time-dependent manner, peaking in cells isolated from mice that had been dosed with KGF 48 h before PBS challenge and remaining similar to PBS control levels in those given KGF 120 h before PBS challenge (Fig. 4*B*). The percentage of AECII that were infected (based on IAV-NP staining) also peaked in dispersed lung cells from mice that had been pretreated with KGF 48 h before infection and remained near PBS control levels in mice given KGF 120 h before delivery of the inoculum (Fig. 4*C*). The mean channel fluorescence (MCF), reflecting viral burden per cell, followed a similar pattern, peaking in cells harvested at 48 h after KGF and remaining close to PBS control levels in cells harvested at 120 h post KGF (Fig. 4*D*). The correlation between peak AECII proliferation and peak AECII infectivity suggests mitogenically stimulated cells are more susceptible to infection.

KGF Produces a Time-Dependent Increase in ex Vivo IAV Infection of AECII that Correlates with Their Proliferative Tone. We conducted ex vivo experiments to examine the role of the mitogenic effects of

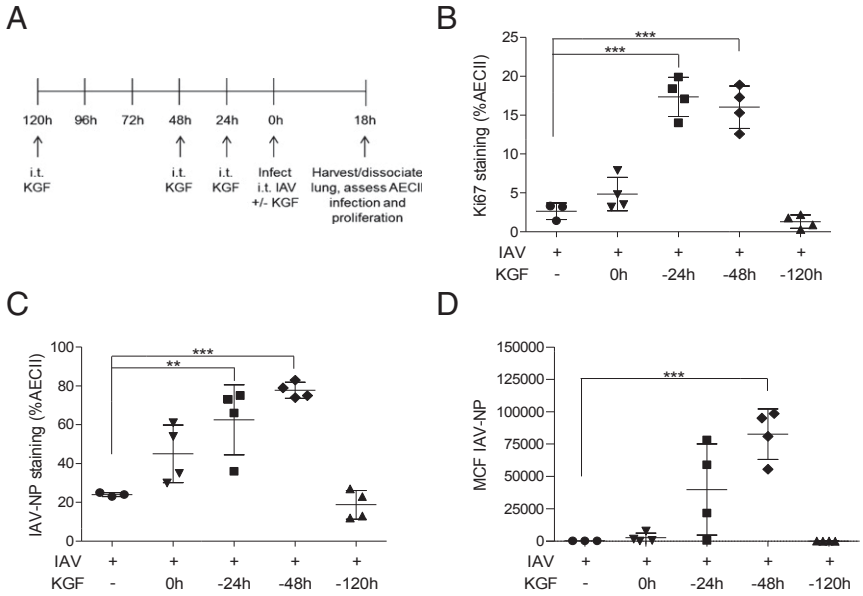

Fig. 4. KGF enhances AECII proliferation and susceptibility to IAV infection. Mice were treated with i.t. KGF (5 mg/kg) 0, 24, 48, or 120 h before IAV infection. Twenty-four hours after challenge with IAV, lungs were harvested and dissociated and dispersed-lung cells were stained with antibody to pro SP-C, IAV-NP, and Ki67 and analyzed by flow cytometry. (*A*) Experimental timeline for *B*–*D* is shown. (*B*) Percentage of pro SP-C–positive cells that also expressed the proliferation marker Ki67 was determined. (*C*) Percentage of pro SP-C–positive cells that were infected with IAV was determined by measuring IAV-NP staining. (*D*) Mean channel fluorescence (MCF) of IAV-NP staining in pro SP-C–positive cells are shown (n = 4/group). $^{**}P < 0.01$; $^{***}P < 0.001$.

KGF on the cell autonomous susceptibility of AECII to IAV infection. AECII were isolated from mice that had been treated with i.t. KGF at 24, 48, or 120 h before and cultured ex vivo with IAV at a multiplicity of infection of 10 in media or media alone (RPMI with 5% FBS) for 18 h (Fig. 5*A*). The cells were then washed, fixed, and stained with anti–IAV-NP, anti-pro SP-C, and anti-Ki67. In AECII isolated at various points after KGF administration, the percentage of AECII that were proliferating based on Ki67 staining rose at 24 h, peaked at 48 h, and returned to near baseline by 120 h post KGF (Fig. 5*B*). The percentage of AECII that were infected after ex vivo IAV incubation was also highest in cells harvested 48 h after in vivo KGF treatment and remained near baseline levels in the cells harvested at 120 h post KGF (Fig. 5*C*). The MCF per cell for IAV-NP followed a similar pattern, peaking in cells harvested at 48 h post KGF and returning to baseline in cells harvested at 120 h after KGF (Fig. 5*D*). Although these analyses revealed an increased percentage of infected AECII and an increased viral burden per AECII (based on mean channel fluorescence) that was associated with the peak in AECII proliferation, these data are correlative and an additional ex vivo experiment was conducted to better establish a causal relationship between proliferation and infectious susceptibility. In AECII harvested 48 h after in vivo KGF administration and infected with IAV ex vivo, the mean fluorescence intensity of IAV-NP staining was greater in the Ki67 high (proliferating) than the Ki67 low (nonproliferating) population, consistent with preferential infection or viral replication in cycling cells (Fig. 5*E*). The peak in expression of viral protein M1 in the lysates of isolated AECII infected with IAV ex vivo also occurred in AECII that were isolated 48 h after in vivo KGF challenge, consistent with greater susceptibility of cycling AECII to IAV infection compared with quiescent cells (Fig. 5 *F* and *G*).

Rapamycin Inhibits KGF-Induced Increases in Mortality, Proliferation, and Viral Susceptibility in Vivo. KGF is known to signal through the MAPK and PI3K/Akt/mTOR pathway. Experiments were conducted to determine whether KGF-induced changes in proliferative tone of AECII could be inhibited with the mTOR inhibitor, rapamycin, in vivo. Mice were treated with once-daily i.p. rapamycin (1 mg/kg) or vehicle control for 4 d before i.t. inoculation with PBS, PBS containing KGF (5 mg/kg) or PBS containing KGF with or without IAV. Lungs were inflation-fixed with formalin at 24 h after i.t. challenge, sectioned and stained with an antibody directed against ribosomal S6 protein phosphorylated at position Ser-235/236. Blinded semiquantitative immunohistochemical analysis revealed a rapamycin-inhibitable increase in phospho-S6 staining of the pulmonary parenchyma in the IAV+KGF group compared with IAV alone, (Fig. 6*A*). Single-cell suspensions were prepared from whole-lung homogenates 48 h after KGF inoculation with or without rapamycin pretreatment of the animals. The dispersed cells were then washed, fixed, and stained with anti-pro SP-C, anti–phospho-S6, and anti-Ki67. The percentage of AECII that were proliferating based on Ki67 staining increased more than sevenfold from 2% to 14% in the KGF inoculated mice, relative to mice given only PBS. Rapamycin pretreatment for 4 d before KGF challenge blocked the proliferative response to KGF (Fig. 6*B*). We next conducted experiments to determine whether KGF-induced enhancement of AECII infectivity could be inhibited with rapamycin in vivo. Mice were treated with rapamycin (1 mg/kg) for 4 d before i.t. inoculation with IAV ± KGF. Single-cell suspensions were prepared from whole-lung homogenates 72 h after infection. The dispersed cells were then washed, fixed, stained with anti–IAV-NP and anti-pro SP-C, and analyzed by flow cytometry. The percentage of AECII that were infected was significantly greater in the KGF-inoculated mice compared with PBS control mice, and the effect was prevented by in vivo pretreatment with rapamycin (Fig. 6*C*). We next conducted experiments to determine whether the observed rapamycin-mediated reduction in AECII proliferation and infectivity attenuated the severity of IAV infection in vivo. We found that rapamycin pretreatment resulted in a significant reduction in KGF-accelerated mortality (Fig. 6*D*; $P < 0.05$), and the KGF-induced increase in the lung tissue levels of the proinflammatory cytokine, IL-6 (Fig. 6*E*). Western blot analysis of IAV-NP levels in whole-lung homogenates harvested 24 h after in vivo infection indicate that rapamycin attenuates IAV

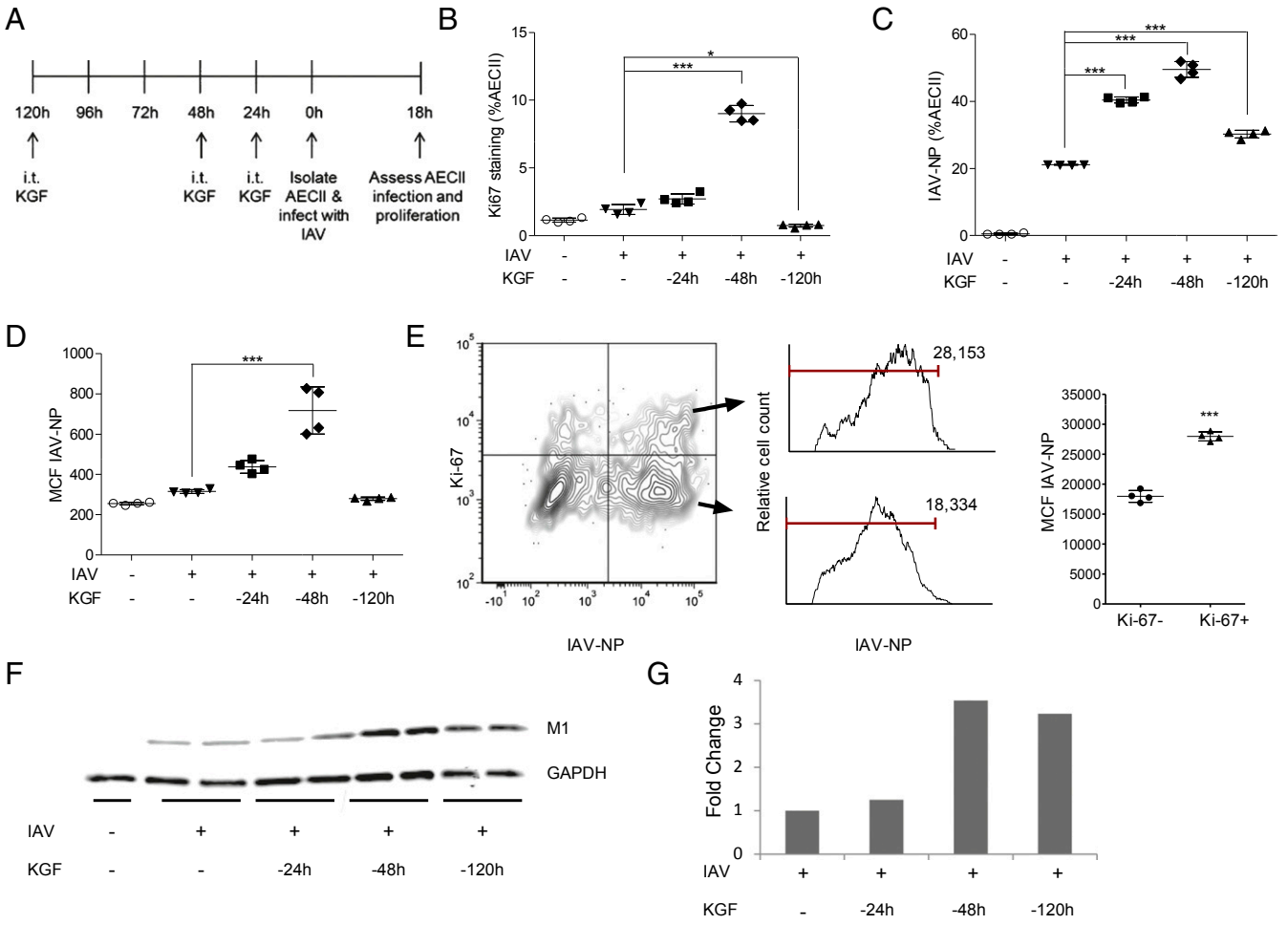

Fig. 5. KGF enhances AECII proliferation and susceptibility to IAV infection, ex vivo. AECII were isolated from mice that were treated with i.t. KGF (5 mg/kg) 24, 48, or 120 h before AECII isolation, incubated with IAV in media or media alone ex vivo for 18 h, fixed and stained with antibodies to Ki67, pro SP-C, and IAV-NP, and analyzed by flow cytometry. (*A*) Experimental timeline for *B*–*D* is shown. (*B*) Percentage of pro SP-C–positive cells that also expressed Ki67 was determined. (*C*) Percentage of pro SP-C–positive cells that stained with IAV-NP are shown. (*D*) MCF of IAV-NP in pro SP-C–positive cells is shown. (*E*) Two-parameter histogram of Ki67 vs. IAV-NP staining of AECII isolated from mice pretreated with KGF 48 h before isolation and infected ex vivo is shown. Cells were harvested and analyzed by flow cytometry at 24 h after infection. Representative IAV-NP staining of Ki67-positive AECII (upper histogram) and Ki67-negative AECII (lower histogram) is shown. IAV-NP mean channel MCF data are shown for one of two independent experiments ($n = 4$). (*F*) Western blot of AECII isolated from mice that were treated with i.t. KGF (5 mg/kg) 24, 48, 120 h before AECII isolation and incubated with IAV in media or media alone ex vivo for 18 h before harvesting. Blots were stained with antibodies to IAV M1 and to GAPDH as a loading control. (*G*) Densitometry analysis of AECII Western blot is shown. $*P < 0.05$; $***P < 0.001$.

production in vivo (Fig. 6*F*). To confirm that KGF-induced viral susceptibility was receptor mediated and to rule out off-target effects, we next examined the effect of the pan-FGFR inhibitor BGJ398 (32) on KGF-enhanced viral susceptibility. A rat AECII primary culture system was developed that was both KGF-responsive and permissive to infection with the IAV strain used in this study. We found that both inhibition of FGF receptor with BGJ398 and mTOR inhibition with sirolimus blocked KGF-induced IAV susceptibility (Fig. S2 *C* and *D*). These data suggest that enhancement of IAV infection and/or replication by KGF, which is known to signal through multiple pathways including Jak/Stat, MAPK, and PI3K, can be at least partially inhibited by targeted blockade at two points within the FGFR/Akt/PI3K/mTOR pathway.

Discussion

This study was initially designed to examine the therapeutic potential of KGF, a potent pulmonary epithelial mitogen that is known to promote expression of innate immune proteins with anti-IAV actions, including the collectins SP-A and SP-D. We were surprised to find that intrapulmonary instillation of KGF in mice worsened IAV-induced mortality, increased pulmonary viral load and inflammatory tone, and accelerated the spread of IAV from the conducting airways to the alveolar compartment. KGF also directly enhanced in vivo susceptibility of AECII to IAV infection in a manner that correlated with their proliferative state. The finding that AECII isolated from KGF-pretreated mice were also more permissive to ex vivo IAV infection suggests that cell autonomous mechanisms, rather than a more global effect on host immunity, are a key driver of AECII infectious susceptibility. These data suggest that the mitogenic tone of AECII in the lung is a potential host risk factor to be considered in the approach to prophylaxis and clinical management of IAV and may be a potential therapeutic target for IAV pneumonia.

Influenza infects airway epithelial cells and Clara cells of the distal conducting airway. At the level of the alveolus, alveolar macrophages, AECI and AECII cells can all be infected with IAV, but among these, AECII are selectively targeted and uniquely capable of sustaining a productive infection (33–36). IAV infection of the pulmonary parenchyma results in loss of expression of SP-C, consistent with reduction in viability and

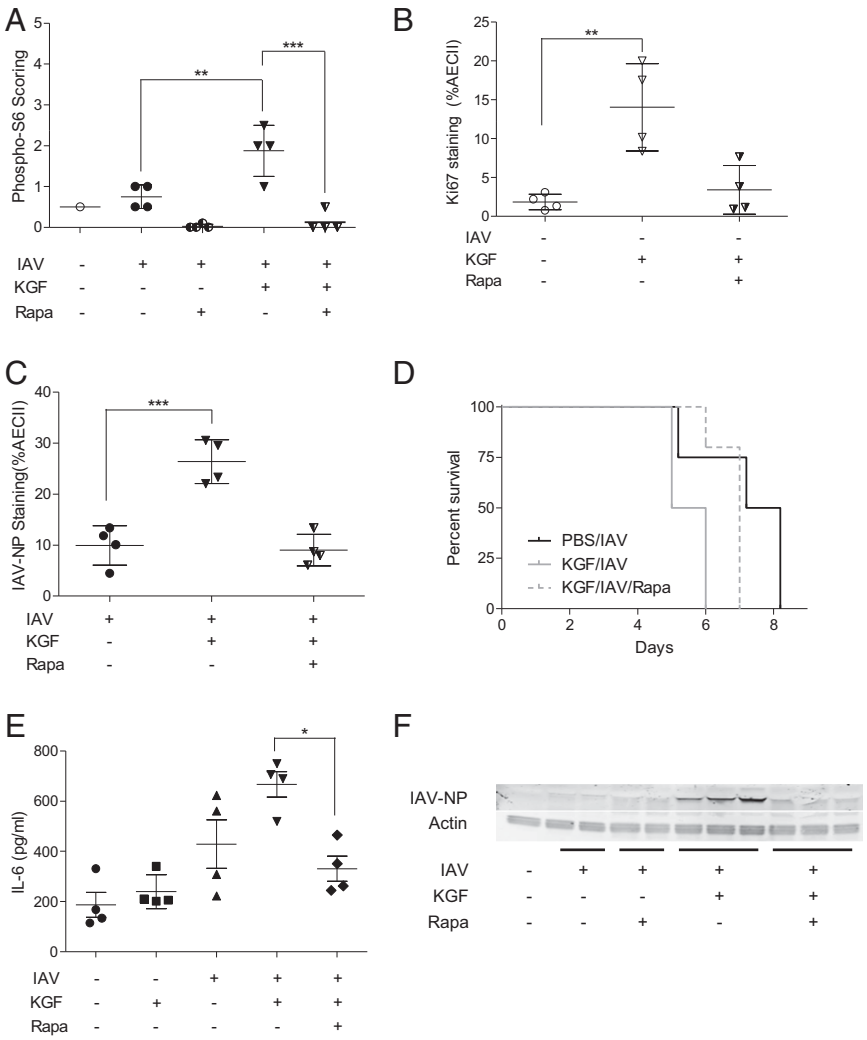

Fig. 6. Rapamycin inhibits KGF-induced mortality, proliferation, cytokine expression, and susceptibility to IAV infection, in vivo. Mice were pretreated with i.p. rapamycin for 4 d before i.t. administration of PBS alone or PBS containing KGF (5 mg/kg) with and without IAV. (*A*) Twenty-four hours after inoculation, immunohistochemical staining for phospho-S6 was performed on lung sections and scored using a semiquantitative scale in a blinded manner. (*B*) Forty-eight hours after challenge with KGF, lungs were harvested and dissociated, and dispersed lung cells were stained with antibodies to pro SP-C, phospho-S6, and Ki67 and examined by flow cytometry to determine the percentage of pro SP-C + Ki67-positive cells. (*C*) Seventy-two hours after challenge with KGF, lungs were harvested and dissociated, and dispersed lung cells were stained with antibody to pro SP-C and IAV-NP and examined by flow cytometry to determine the percentage of pro SP-C + IAV-NP positive cells. (*D*) Vital status was monitored over the course of 9 d after IAV infection of rapamycin-pretreated mice and controls ($P < 0.05$ for KGF/IAV vs. KGF/IAV/rapa). (*E*) IL-6 levels were measured by ELISA in whole-lung homogenates at 48 h after infection. (*F*) Western blotting was performed on whole-lung homogenates isolated 24 h after IAV infection. Blots were stained with antibodies to IAV-NP and to actin as a loading control. ***$P < 0.001$; **$P < 0.01$; *$P < 0.05$.

differentiated functions of AECII cells (37, 38). This consequence of IAV infection critically affects alveolar homeostasis through loss of AECII roles in regulating innate immune responses, lowering surface pressures through surfactant synthesis and secretion, and disruption of lumenal fluid and electrolyte balance. Pathological evaluations of lung samples from cases of fatal influenza uniformly reveal evidence for diffuse alveolar damage, consistent with direct injury to the alveolar epithelium as a mechanism of death in influenza pneumonia (39).

The spread of IAV from the epithelium of the conducting airway to the alveolar epithelium is therefore a pivotal event in the pathogenesis of fatal influenza pneumonia. Multiple host factors align to impede this transition, including physical defenses such as mucociliary clearance, humoral defenses including antibodies, cellular defenses such as natural killer cells, and inhibition of proteolytic activation of the virus (40). To explore the mechanism of the KGF effect, we first considered the possibility that the mitogen was enhancing mortality in IAV-infected mice by inducing a lethal hyper-inflammatory response. We found that KGF augmentation of IAV-induced inflammation was quite modest and consistent with a slightly higher viral burden (Fig. 1 and 2) induced by the growth factor. We next considered that the strong mitogenic effect of KGF might enhance the susceptibility of AECII directly. The effect of KGF on IAV-induced mortality was time- and dose-dependent, maximal at 5 mg/kg KGF. Low- and high-power microscopic analysis of lung sections from IAV-infected mice stained with antibodies to IAV-NP revealed that KGF administration accelerated spread of infection from the airway to the lung parenchyma, producing peribronchiolar rosettes of IAV-NP positivity corresponding to secondary lobules by 48 h and much more intense and diffuse overall staining by 120 h. The timing of i.t. KGF administration relative to i.t. IAV challenge had a significant effect on AECII infection. The numbers of AECII infected and the mean fluorescence intensity

corresponding to the burden of IAV per cell were both at their greatest when the IAV challenge occurred 48 h after i.t. KGF, which was also the point with greatest AECII proliferation based on Ki67 staining. Both the proliferative effects of KGF and the susceptibility of IAV infection returned to baseline by 120 h, consistent with the observation that there is no enhanced mortality effect when KGF is administered to mice 120 h before IAV challenge (Fig. 1*C*). To assess the effects of KGF on susceptibility of AECII to IAV infection removed from any influence of the host immune system, we performed experiments in which KGF was delivered in vivo but IAV infection was conducted on isolated AECII ex vivo. Again, we saw that AECII were most vulnerable when infected 48 h after KGF administration, and that susceptibility returned to baseline by 120 h after KGF exposure. In the cells that were IAV infected 48 h after in vivo KGF administration, the proliferating cells (Ki67 high) had a higher viral burden per cell than the nonproliferating (Ki67 low) cells. Consistent with that finding, the expression of the viral protein M1 in IAV-infected AECII also peaked at 48 h post KGF stimulation, based on Western blot analysis of cell lysates from AECII harvested at multiple points after KGF administration and infected ex vivo.

We find that the molecular mechanism or mechanisms of KGF-enhanced mortality and susceptibility of AECII cells involves activation of the PI3K/Akt/mTOR pathway that is known to facilitate endocytosis and viral replication, in that both the AECII proliferative response (Fig. 6 *A* and *B*) and burden of IAV infection (Fig. 6 *C* and *F*) were diminished by pretreatment with rapamycin. In addition, rapamycin blocked both KGF-enhanced IL-6 production and KGF-enhanced mortality. It is interesting to note that a small randomized clinical trial of corticosteroids + rapamycin vs. corticosteroids alone in patients with severe H1N1 IAV demonstrated benefit from the combination therapy (41). It is tempting to speculate that rapamycin and other PI3K/Akt/mTOR pathway inhibitors might have prophylactic or therapeutic utility in IAV.

Genomewide RNA interference screening has identified the cognate receptor for KGF, FGFR2, as one of 23 proteins required for viral entry and the PI3K/Akt/mTOR, MAPK, and IP-3 PKC signaling pathways as most essential for early-stage IAV replication (42). There is also evidence that IAV uses molecular mimicry and other mechanisms to activate cellular signaling pathways to augment its own internalization and proliferation. Binding and clustering of the epidermal growth factor receptor by IAV results in autophosphorylation of the receptor. This signaling event enhances viral internalization by a PI3K/mTOR/AKT pathway, possibly driven by a Trojan horse-like mechanism in which IAV is towed into the cell while bound to epidermal growth factor receptor glycans (43). In addition, it is known that the NS1 protein produced by IAV binds to the p85β subunit of PI3K to induce PI3K activity in infected cells (44). Finally, pharmacological intervention with inhibitors of PI3K and rapamycin block IAV replication in vitro, which is consistent with a role for the PI3K/Akt/mTOR pathway in IAV infection (33, 45).

Our data demonstrate a correlation between increased susceptibility to influenza infection and increased proliferation in AECII. On the basis of these data, it occurs to us that the remarkably quiescent state of the AECII in the healthy host, in which less than 1% of AECII are proliferating at any given time, may function as a passive host defense strategy to limit the intrapulmonary spread of IAV infection. The perspective that AECII infection is a pivotal event that determines outcome in influenza infection and that proliferation-dependent AECII susceptibility may be modulated by clinical states such as lung injury raises interesting and potentially clinically relevant questions about our approach to the care of the IAV-infected patient. For instance Sawicki et al. demonstrated almost 50 y ago that exposure of mice to 50% oxygen markedly accelerates IAV- and influenza B virus-induced mortality (46). We speculate that cavalier use of excessive levels of supplemental oxygen in IAV-infected patients may enhance AECII proliferation (as it is known to do in rodents) and promote progression to viral pneumonia (47, 48).

Other host susceptibility states that are associated with influenza mortality are also of interest. It is known that the fraction of AECII that are proliferating is much higher in infants (49), which could potentially explain their increased susceptibility to IAV infection. Similarly, cigarette smoking is known to enhance susceptibility to IAV infection in humans (50, 51), perhaps through increasing pulmonary epithelial cell proliferation, as has been reported in rats (52). It occurs to us that the enhanced mortality of influenza in pregnancy could also be related to hormonal influences on the mitogenic tone of AECII cells, although we can find no human or animal data to support this notion. Finally, patients with hematologic cancer treated with KGF for stomatitis (53) may be at enhanced risk for lethal consequences from exposure to IAV or other viruses. Consistent with this notion, KGF treatment has been reported to worsen infection caused by anorectal papillomavirus (54).

In conclusion, we found that mitogenic stimulation by the lung pulmonary epithelial mitogen KGF hastens spread of influenza to the alveolar epithelium and the subsequent development of lethal influenza pneumonia in mice. We propose that the elevated mitogenic tone of the lung may be an overlooked host risk factor that can be exploited by IAV and that should be considered in relation to the enhanced risk for poor outcomes often seen in vulnerable groups. Future therapeutic implications from this line of investigation could include more judicious use of supplemental oxygen in patients suspected to have IAV, careful attention of IAV vaccination status in patients who may require KGF treatment for mucositis, and the use of short-course antiproliferative therapies targeting epithelial mTOR activation in patients with early but rapidly progressive IAV pneumonia.

Materials and Methods

Mouse Models of IAV Infection. Animal studies were conducted with 10–16-wk-old female DBA/2J mice (The Jackson Laboratory). Mice were lightly anesthetized with isoflurane and i.t. inoculated (via the oropharyngeal route) with the SP-D–sensitive hybrid IAV strain, WSNHAnc-Asp225Gly (hereafter referred to as IAV), grown in Madin-Darby canine kidney cells (20, 54), together with 5 mg/kg KGF in 50 μL Dulbecco's PBS. Animals were monitored daily for vital status. For some experiments, lungs were harvested at 24, 48, and 72 h postviral infection, and the tissues were homogenized in Dulbecco's PBS without Ca^{2+} and Mg^{2+}. After centrifugation at 3,000 × *g* for 10 min, the clarified supernatant was collected, aliquoted, and stored at −80 °C In other studies, AECII were isolated 0, 24, 48, or 120 h after i.t. administration of KGF (5 mg/kg), KGF/IAV, or PBS. All animals were maintained in a specific pathogen-free facility and were handled according to a protocol approved by the University of Cincinnati Institutional Animal Care and Use Committee.

Quantification of Viral Particles. Total RNA was isolated from mouse lung homogenates using the QIAamp Viral RNA Mini Kit (Qiagen). Viral RNA was purified by the Viral RNA Spin Protocol (Qiagen), using the Bio-Rad One-Step RT-PCR enzyme mix (Bio-Rad), and the Influenza-A Virus Detection Kit (AD502, iGentBio).

Histological Assessment of Viral Infection. The trachea was cannulated and lungs were inflation-fixed with neutral-buffered 10% formalin (Fisher Scientific) at a pressure of 25 cm H_2O. The lungs were harvested and immersed in 10% formalin overnight, embedded in paraffin, cut into 5-μm sections, and mounted on Trubond 380 adhesive microscope slides (Tru Scientific). Endogenous peroxidase activity was quenched with 0.3% hydrogen peroxide in methanol; sections were blocked with 15% normal goat serum and incubated with rabbit anti-IAV NP antibody (Virostat; 1:1,500 dilution) overnight at 4 °C. Slides were developed by incubation with biotin-labeled goat anti-rabbit IgG secondary antibody (1:750 dilution) and avidin-peroxidase-dependent (Vector Laboratories) oxidation of diaminobenzidine. A blinded analysis of the burden of viral infection in conducting airways and lung parenchyma was performed

by scoring the intensity of immunohistochemical staining for IAV-NP, using a semiquantitative scale [i.e., −1 (least) to 4 (most)].

Cytokine Determination. Inflammatory cytokines in clarified supernatants of whole-lung homogenates were measured by ELISA, according to the manufacturer's instructions (R&D Systems). Multianalyte studies of BAL fluid and serum were conducted by ELISA, using Milliplex Multiplex kits (Millipore) according to the manufacturer's protocol. Concentrations were calculated from standard curves, using recombinant protein standards and expressed in picograms per milliliter.

Preparation of Dispersed Cells from Whole Lung. Explanted lungs were instilled with 5,000 caseinolytic units (c.u.)/mL dispase (BD Biosciences) via the i.t. route and then immersed (Worthington Biochemicals) in 3 mL ice cold dispase (5,000 c.u.)/mL containing 50 U/mL DNase. Lung tissues were then processed in a gentleMACS Dissociator according to manufacturer's instructions (Miltenyi Biotec), and cell suspensions were passed through a 40-μm filter before washing with Dulbecco's PBS and subsequent analysis.

Flow Cytometry and Identification of Epithelial Cell Subtypes. Fixation of dispersed lung cells was accomplished either in sequential steps, using ammonium chloride lysis solution (Stemcell Technologies) followed by paraformaldehyde (1.6% for 10 min), or in a single step, using eBioscience fix/lysis reagent. Cells were washed and resuspended in 70% methanol/FACS buffer overnight before washing and incubation with antibodies. AECII and pulmonary epithelial cells were identified by staining with anti-pro SPC (Seven Hills Bioreagents) and anti-CD326 (clone G8.8; eBioscience), respectively. Alveolar macrophages were identified using antibodies to F4/80 (clone BM8; eBioscience) and CD11c (clone N418; eBioscience). Influenza virus was detected using an antibody to IAV-NP (clone D67J; Thermo Fisher Pierce). Proliferative status was determined using the Ki67 antibody (clone SOLA15; eBioscience). Compensation for fluorescence overlap and background fluorescence was accomplished using fluorescence minus one controls. Samples were run on a FACS LSRII, using four lasers (325, 405,488, and 633 nm) (Becton Dickenson). Data were analyzed using FCS Express flow cytometry software.

Isolation, Enrichment, and IAV Infection of AECII. Ex vivo IAV infectivity assays were performed with AECII isolated as previously described (30) 0, 24, 48, and 120 h after i.t. administration of PBS or 5 mg/kg KGF. Briefly, saline-perfused lungs were instilled with 5,000 c.u. dispase via the i.t. route, followed by 0.5 mL melted agarose. The lungs were immersed in a 3-mL solution containing 5,000 c.u./mL dispase, incubated at 37 °C for 45 min, and gently teased apart in RPMI media containing DNase. The cell suspension was filtered through 40 μm membranes and panned on plates coated with anti-CD45 and CD16/32 (BD Biosciences) to remove immune cells and fibroblasts. After RBC lysis, an aliquot of the cell suspension was spun onto slides (Thermo-Shandon) and stained with pro-SPC antibody and Trypan blue to determine purity and viability of AECII, respectively. Cell suspensions that were verified to be at least 85% pure AECII were then plated in 24-well plates at a density of 2.5×10^5 cells/well, and incubated with 2.5×10^4 IAV particles in media (RPMI with 5% FBS) or media alone for 18 h at 37 °C in a 5% CO_2 atmosphere. Cells were harvested, washed, fixed, permeabilized, and stained with antibodies before analysis by flow cytometry, as described earlier. For Western blot analysis, cell lysates were prepared in RIPA lysis buffer with protease and phosphatase inhibitors. Equal amounts of clarified supernatants were size-fractionated on 4–20% SDS/PAGE gels and transferred to nitrocellulose membranes. The blots were probed with IAV-M1 antibody (ABD-Serotec), followed by secondary antibodies conjugated with IRDye 800CW linked to goat anti-rabbit or goat anti-mouse (Li-Cor). GAPDH was used as a loading control. Images were captured using a Li-Cor Odyssey per manufacturer's instructions.

ACKNOWLEDGMENTS. We are grateful to Dr. Donald Smee, Utah State University, for providing the WSNHAnc-Asp225Gly strain of IAV. We thank Swedish Orphan Biovitrum for the kind gift of KGF. This work was supported by National Institute of Allergy and Infectious Diseases Grant P01AI083222 (to F.X.M.), National Institute of Environmental Health Sciences Center for Environmental Genetics Grant P30-ES006096 (to F.X.M.), and The Carespring Foundation (to F.X.M.). K.L.H. and M.R.W. were supported by National Heart, Lung, and Blood Institute Grant HL069031 and National Institute of Allergy and Infectious Diseases Grant P01AI083222.

1. Crowther JE, et al. (2004) Pulmonary surfactant protein a inhibits macrophage reactive oxygen intermediate production in response to stimuli by reducing NADPH oxidase activity. *J Immunol* 172:6866–6874.
2. Zhou H, et al. (2012) Hospitalizations associated with influenza and respiratory syncytial virus in the United States, 1993-2008. *Clin Infect Dis* 54:1427–1436.
3. Russell CA, et al. (2008) The global circulation of seasonal influenza A (H3N2) viruses. *Science* 320:340–346.
4. Monto AS, Gravenstein S, Elliott M, Colopy M, Schweinle J (2000) Clinical signs and symptoms predicting influenza infection. *Arch Intern Med* 160:3243–3247.
5. Short KR, Kroeze EJ, Fouchier RA, Kuiken T (2014) Pathogenesis of influenza-induced acute respiratory distress syndrome. *Lancet Infect Dis* 14:57–69.
6. Kourtis AP, Read JS, Jamieson DJ (2014) Pregnancy and infection. *N Engl J Med* 371:1077.
7. Centers for Disease Control and Prevention (CDC) (2010) Estimates of deaths associated with seasonal influenza — United States, 1976-2007. *MMWR Morb Mortal Wkly Rep* 59:1057–1062.
8. Murin S, Bilello KS (2005) Respiratory tract infections: Another reason not to smoke. *Cleve Clin J Med* 72:916–920.
9. Myles PR, et al.; Influenza Clinical Information Network (FLU-CIN) (2012) Predictors of clinical outcome in a national hospitalised cohort across both waves of the influenza A/H1N1 pandemic 2009-2010 in the UK. *Thorax* 67:709–717.
10. Liang Y, et al. (2014) PM2.5 in Beijing - temporal pattern and its association with influenza. *Environ Health* 13:102.
11. Hilleman MR (2002) Realities and enigmas of human viral influenza: Pathogenesis, epidemiology and control. *Vaccine* 20:3068–3087.
12. Whitley RJ, Monto AS (2006) Prevention and treatment of influenza in high-risk groups: Children, pregnant women, immunocompromised hosts, and nursing home residents. *J Infect Dis* 194:S133–S138.
13. Bouvier NM, Palese P (2008) The biology of influenza viruses. *Vaccine* 26:D49–D53.
14. Steinhauer DA (1999) Role of hemagglutinin cleavage for the pathogenicity of influenza virus. *Virology* 258:1–20.
15. Cros JF, Palese P (2003) Trafficking of viral genomic RNA into and out of the nucleus: Influenza, Thogoto and Borna disease viruses. *Virus Res* 95:3–12.
16. Kash JC, Goodman AG, Korth MJ, Katze MG (2006) Hijacking of the host-cell response and translational control during influenza virus infection. *Virus Res* 119:111–120.
17. Nayak DP, Hui EK, Barman S (2004) Assembly and budding of influenza virus. *Virus Res* 106:147–165.
18. Wagner R, Matrosovich M, Klenk HD (2002) Functional balance between haemagglutinin and neuraminidase in influenza virus infections. *Rev Med Virol* 12:159–166.
19. LeVine AM, Hartshorn K, Elliott J, Whitsett J, Korfhagen T (2002) Absence of SP-A modulates innate and adaptive defense responses to pulmonary influenza infection. *Am J Physiol Lung Cell Mol Physiol* 282:L563–L572.
20. Crouch E, et al. (2011) Mutagenesis of surfactant protein D informed by evolution and x-ray crystallography enhances defenses against influenza A virus in vivo. *J Biol Chem* 286:40681–40692.
21. Li G, et al. (2002) Surfactant protein-A–deficient mice display an exaggerated early inflammatory response to a beta-resistant strain of influenza A virus. *Am J Respir Cell Mol Biol* 26:277–282.
22. Hawgood S, et al. (2004) Pulmonary collectins modulate strain-specific influenza a virus infection and host responses. *J Virol* 78:8565–8572.
23. Vigerust DJ, et al. (2007) N-linked glycosylation attenuates H3N2 influenza viruses. *J Virol* 81:8593–8600.
24. LeVine AM, Whitsett JA, Hartshorn KL, Crouch EC, Korfhagen TR (2001) Surfactant protein D enhances clearance of influenza A virus from the lung in vivo. *J Immunol* 167:5868–5873.
25. Barazzone C, et al. (1999) Keratinocyte growth factor protects alveolar epithelium and endothelium from oxygen-induced injury in mice. *Am J Pathol* 154:1479–1487.
26. Guo J, et al. (1998) Intravenous keratinocyte growth factor protects against experimental pulmonary injury. *Am J Physiol* 275:L800–L805.
27. Deterding RR, et al. (1997) Prevention of bleomycin-induced lung injury in rats by keratinocyte growth factor. *Proc Assoc Am Physicians* 109:254–268.
28. Yano T, Deterding RR, Simonet WS, Shannon JM, Mason RJ (1996) Keratinocyte growth factor reduces lung damage due to acid instillation in rats. *Am J Respir Cell Mol Biol* 15:433–442.
29. Panos RJ, Bak PM, Simonet WS, Rubin JS, Smith LJ (1995) Intratracheal instillation of keratinocyte growth factor decreases hyperoxia-induced mortality in rats. *J Clin Invest* 96:2026–2033.
30. Wu H, Suzuki T, Carey B, Trapnell BC, McCormack FX (2011) Keratinocyte growth factor augments pulmonary innate immunity through epithelium-driven, GM-CSF-dependent paracrine activation of alveolar macrophages. *J Biol Chem* 286:14932–14940.
31. Gardner JC, et al. (2016) Keratinocyte growth factor supports pulmonary innate immune defense through maintenance of alveolar antimicrobial protein levels and macrophage function. *Am J Physiol Lung Cell Mol Physiol* 310:L868–L879.
32. Guagnano V, et al. (2011) Discovery of 3-(2,6-dichloro-3,5-dimethoxy-phenyl)-1-6-[4-(4-ethyl-piperazin-1-yl)-phenylamino]-pyrimidin-4-yl-1-methyl-urea (NVP-BGJ398), a potent and selective inhibitor of the fibroblast growth factor receptor family of receptor tyrosine kinase. *J Med Chem* 54:7066–7083.
33. Weinheimer VK, et al. (2012) Influenza A viruses target type II pneumocytes in the human lung. *J Infect Dis* 206:1685–1694.
34. van Riel D, et al. (2006) H5N1 virus attachment to lower respiratory tract. *Science* 312:399.
35. van Riel D, et al. (2007) Human and avian influenza viruses target different cells in the lower respiratory tract of humans and other mammals. *Am J Pathol* 171:1215–1223.
36. Shinya K, et al. (2006) Avian flu: Influenza virus receptors in the human airway. *Nature* 440:435–436.

37. Kumar PA, et al. (2011) Distal airway stem cells yield alveoli in vitro and during lung regeneration following H1N1 influenza infection. *Cell* 147:525–538.
38. Hofer CC, Woods PS, Davis IC (2015) Infection of mice with influenza A/WSN/33 (H1N1) virus alters alveolar type II cell phenotype. *Am J Physiol Lung Cell Mol Physiol* 2015;308:L628–L638.
39. Taubenberger JK, Morens DM (2008) The pathology of influenza virus infections. *Annu Rev Pathol* 3:499–522.
40. Tripathi S, White MR, Hartshorn KL (2015) The amazing innate immune response to influenza A virus infection. *Innate Immun* 21:73–98.
41. Wang CH, et al. (2014) Adjuvant treatment with a mammalian target of rapamycin inhibitor, sirolimus, and steroids improves outcomes in patients with severe H1N1 pneumonia and acute respiratory failure. *Crit Care Med* 42:313–321.
42. König R, et al. (2010) Human host factors required for influenza virus replication. *Nature* 463:813–817.
43. Eierhoff T, Hrincius ER, Rescher U, Ludwig S, Ehrhardt C (2010) The epidermal growth factor receptor (EGFR) promotes uptake of influenza A viruses (IAV) into host cells. *PLoS Pathog* 6:e1001099.
44. Hale BG, Jackson D, Chen YH, Lamb RA, Randall RE (2006) Influenza A virus NS1 protein binds p85beta and activates phosphatidylinositol-3-kinase signaling. *Proc Natl Acad Sci USA* 103:14194–14199.
45. Ehrhardt C, et al. (2006) Bivalent role of the phosphatidylinositol-3-kinase (PI3K) during influenza virus infection and host cell defence. *Cell Microbiol* 8:1336–1348.
46. Sawicki L, Baron S, Isaacs A (1961) Influence of increased oxygenation on influenza virus infection in mice. *Lancet* 2:680–682.
47. Adamson IY, Bowden DH (1974) The type 2 cell as progenitor of alveolar epithelial regeneration. A cytodynamic study in mice after exposure to oxygen. *Lab Invest* 30: 35–42.
48. Evans MJ, Hackney JD (1972) Cell proliferation in lungs of mice exposed to elevated concentrations of oxygen. *Aerosp Med* 43:620–622.
49. Kauffman SL (1980) Cell proliferation in the mammalian lung. *Int Rev Exp Pathol* 22: 131–191.
50. Kark JD, Lebiush M (1981) Smoking and epidemic influenza-like illness in female military recruits: A brief survey. *Am J Public Health* 71:530–532.
51. Kark JD, Lebiush M, Rannon L (1982) Cigarette smoking as a risk factor for epidemic a(h1n1) influenza in young men. *N Engl J Med* 307:1042–1046.
52. Wells AB, Lamerton LF (1975) Regenerative response of the rat tracheal epithelium after acute exposure to tobacco smoke: A quantitative study. *J Natl Cancer Inst* 55: 887–891.
53. Spielberger R, et al. (2004) Palifermin for oral mucositis after intensive therapy for hematologic cancers. *N Engl J Med* 351:2590–2598.
54. Schroeder T, Zohren F, Saure C, Kobbe G, Haas R (2009) Palifermin, a recombinant human keratinocyte growth factor, triggers reactivation of anogenital human papillomavirus infection in a HIV-positive patient with diffuse large cell B-cell non-Hodgkin lymphoma. *Bone Marrow Transplant* 44:823–824.